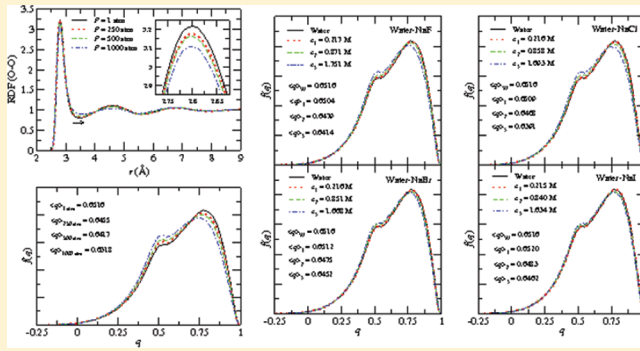


# Mapping Structural Perturbations of Water in Ionic Solutions

N. Galamba\*

Grupo de Física-Matemática da Universidade de Lisboa, Av. Prof. Gama Pinto 2, 1649-003 Lisboa, Portugal

**ABSTRACT:** The structure of water in sodium halide aqueous solutions at different concentrations is studied through molecular dynamics. Emphasis is placed on the extent of ionic-induced changes in the water structure, and the concept of kosmotropes/chaotropes is probed, in terms of perturbations to the tetrahedral H-bond network of water. The results show that at low salt concentrations, the halide anions slightly increase the tetrahedrality of the H-bond network of water in the anionic second hydration shell and  $I^-$  is found to be the strongest kosmotrope, contrary to its structure breaker reputation. The sodium cation in turn induces a significant loss of tetrahedrality in the second cationic hydration shell. At higher concentrations, the dominant disruptive effect of  $Na^+$  cancels the anionic effects, even in the anionic second hydration shell. According to a kosmotropes/chaotropes classification of ions, based on the tetrahedrality of the H-bond network of water, halide anions are therefore weak kosmotropes, while  $Na^+$  is a strong chaotrope. However, if this classification is applied to the salts, rather than to the ions, all of the sodium halides are classified as structure breakers even at low concentrations. Further, the effect of pressure on the tetrahedrality of the H-bond network of water is found to be similar to the average effect of the dissolved salts. The present results indicate that the classification of ions in kosmotropes/chaotropes in terms of long-range perturbations to the tetrahedral H-bond network of water is not correlated to the position of the ions in the respective Hofmeister series.



## I. INTRODUCTION

The structural and dynamic perturbations of the hydrogen-bond (H-bond) network of water induced by different ionic species play a critical role in many chemical and biological processes.<sup>1–6</sup> The study of ionic hydration has been the object of innumerable experimental<sup>7–25</sup> and simulation<sup>24,26–45</sup> works, providing information on the water structure and dynamics inside<sup>5</sup> and beyond the first ionic hydration shell.<sup>2,4,6</sup> Nonetheless, the hydration of ionic solutes remains intriguing due to the opposite observations regarding the extent of specific ion effects, from which different microscopic pictures of ionic hydration emerged. Thus, although ionic hydration is often discussed with recourse to the concept of kosmotropes/chaotropes, or similarly, ionic structure makers/breakers, this view has been questioned.<sup>1,15,20,46</sup> The divergences between distinct experimental and theoretical results on ionic hydration have raised some fundamental questions, explicitly, the restriction or not, of the perturbations of the H-bond network of water, imputed to ions, to the first hydration shell, or the closely related issue, on the suitability of the concept of ionic kosmotropes/chaotropes, to interpret these perturbations. The answer to the aforementioned questions is key to understanding the molecular origin of phenomena as diverse as the increase of the viscosity of ionic solutions relative to neat water, ionic mobility or the role played by water, outside the first ionic hydration shells, on the solubility of proteins in salt solutions. The latter is further related to the position of cations and anions in the Hofmeister series, which orders ions according to

their ability to precipitate (salt-out) proteins.<sup>47</sup> The current view on the mechanisms underlying protein stability foresees a minor role to bulk water structure, attributing a much more decisive part to ion–protein interactions.<sup>1</sup> Furthermore, it has been argued, based on thermodynamic data and the classic two-state mixture model for water, that the effect of ions on the water structure is not correlated to ionic effects on protein stability.<sup>8</sup>

Ionic-induced modifications of the water structure have been probed through neutron diffraction experiments, putting forward a view where the ability of ions to disrupt the water H-bond network is comparable to the effect of pressure or temperature.<sup>14</sup> More recently, Soper and Weckstrom<sup>21</sup> studied the structure of water in potassium halide solutions, at different concentrations, through neutron diffraction, combined with the method of empirical potential structure refinement (EPSR), concluding that the effect of the halide anions on the water structure beyond the first hydration shell is relatively small. Another neutron diffraction/EPSR study on NaCl and KCl aqueous solutions concluded that the concept of ionic kosmotropes/chaotropes is unsuitable to describe ionic hydration effects.<sup>16</sup> The authors argued that the concept is misleading because some ions, like  $Na^+$ , can tightly coordinate to water in the first hydration shell and disrupt the water

Received: February 13, 2012

Revised: April 5, 2012

Published: April 5, 2012

structure outside the first hydration layer. MD of NaCl aqueous solutions have also suggested a close relation between pressure and salt effects on the water structure, at low temperatures.<sup>38</sup> This was further supported recently by another MD study on NaCl, KCl, and KF salt solutions at normal and supercooled conditions.<sup>42</sup> However, this pressure equivalence was not supported by a MD study on CaCl<sub>2</sub> aqueous solutions at room temperature.<sup>40</sup>

The structure of water in salt solutions has also been studied indirectly by comparing the dynamics of water molecules inside and beyond the first ionic hydration shells. Femtosecond mid-infrared pump probe spectroscopy was used to probe the rotational dynamics of water in different salt aqueous solutions, showing that the orientational-correlation time of water was not affected beyond the first ionic hydration shell.<sup>18,48</sup> This result supports the interpretation that specific ion effects are short ranged and the H-bond network of water outside the first ionic hydration shell is neither enhanced nor disrupted.

Here, the hydration of sodium halides at different concentrations is investigated through MD simulations. The halide anions occupy the following relative positions in the anionic Hofmeister series [F<sup>-</sup> > Cl<sup>-</sup> > Br<sup>-</sup> > I<sup>-</sup>], where I<sup>-</sup> is usually referred to as a chaotrope, on one hand, and a protein denaturant, on the other, and at the left end, F<sup>-</sup> takes upon the role of kosmotrope, salting-out proteins. The chosen counterion, Na<sup>+</sup>, is somewhat of a borderline ion in the cationic Hofmeister series, considered a weak kosmotrope.

One of the problems in discussing specific ion-effects in terms of the concept of structure maker/breaker is the lack of an exact definition as discussed by Soper and Weckstrom.<sup>21</sup> In fact, it has been argued that kosmotropes and chaotropes can disrupt and enhance the structure of water, respectively, contrary to the intuitive meaning of this classification.<sup>27,49</sup> In the present work, we adopt the view that this concept is related exclusively to the effect of ions on the water structure, beyond the ionic first hydration shell. On the other hand, a structure maker is thought to enhance the tetrahedrality of the H-bond network of water and a structure breaker to exert the opposite effect. Thus, we associate this concept only to the hypothetical long-range effects on the water structure and do not consider here the closely related orientational and vibrational dynamics of water in the ionic hydration shells. Notice that we do not assume, in the present analysis, a direct relationship between the entropy of ions (salts) in solution, frequently linked to the concept of kosmotropes/chaotropes, and the measured orientational order of water, in particular because we do not address the problem of water's tetrahedrality perturbation when a vertex (O atom) of a "tetrahedron" in the H-bond network of water is replaced by an ion, that is, the tetrahedrality of water molecules in close interaction with the ions, while entropy changes are associated to the disorder in the first, second, and third ionic hydration shells, as well as in the bulk. Thus, rather, we establish an analogy between the water response to pressure, concerning the tetrahedrality of water's H-bond network, and the tetrahedrality of water in specific regions outside the first ionic hydration shell, in the salt solutions.

## II. METHODS

Molecular dynamics (MD) simulations of Na<sub>n</sub>X<sub>n</sub> with [X = F<sup>-</sup>, Cl<sup>-</sup>, Br<sup>-</sup>, I<sup>-</sup>; n = 1, 4, 8] and 256 water molecules, at 298.15 K and 1 atm, were carried out with the flexible and polarizable force field AMOEBA 04.<sup>50,51</sup> The average concentration and density of the different solutions are reported in Table 1. MD

**Table 1. Number of Ionic Pairs, N, Number Density of Water,  $\langle n \rangle$ , Solution Mass Density,  $\langle \rho \rangle$ , and Concentration,  $c$ , of the AMOEBA Salt Solutions at 298.15 K and 1 atm<sup>a</sup>**

| system | N | c (M) | $\langle n \rangle$ (10 <sup>-2</sup> Å <sup>3</sup> ) | $\langle \rho \rangle$ (g cm <sup>-3</sup> ) |
|--------|---|-------|--|--|
| water  |   |       | 3.338  | 0.9987                                       |
| NaF    | 1 | 0.217 | 3.350  | 1.011  |
|        | 4 | 0.871 | 3.357  | 1.041  |
|        | 8 | 1.751 | 3.374  | 1.083  |
| NaCl   | 1 | 0.216 | 3.329  | 1.009  |
|        | 4 | 0.858 | 3.307  | 1.039  |
|        | 8 | 1.693 | 3.262  | 1.075  |
| NaBr   | 1 | 0.216 | 3.330  | 1.018  |
|        | 4 | 0.851 | 3.282  | 1.069  |
|        | 8 | 1.668 | 3.215  | 1.133  |
| NaI    | 1 | 0.215 | 3.313  | 1.023  |
|        | 4 | 0.840 | 3.239  | 1.095  |
|        | 8 | 1.634 | 3.149  | 1.187  |

<sup>a</sup>The concentrations, from the lowest to the highest, are denoted by  $c_1$ ,  $c_2$ , and  $c_3$  in this Article.

of pure water at 298.15 K and 1, 250, 500, and 1000 atm were also performed for comparison purposes. The MD were carried out with the program Tinker 5.1.<sup>52</sup> The long-range electrostatic interactions were calculated with the Ewald summation. Nonbonded van der Waals interactions and the Ewald real space summation were truncated at  $L/2$ , where  $L$  is the average length of the cubic MD box after equilibration. A modified Beeman algorithm<sup>52,53</sup> was used to integrate the equations of motion with a time-step of 0.5 fs. The starting positions were those of a face centered cubic crystal at the experimental density of water (0.997 g cm<sup>-3</sup>) or a somewhat lower value for the high concentration solutions, with the ions positioned in close contact. The systems were first equilibrated for 150 ps in the (N,V,T) isokinetic<sup>54</sup> environment. This was followed by a (N,P,T) simulation for 300 ps at the same temperature and 1 atm, using the thermostat and barostat of Berendsen.<sup>54</sup> The production was carried out for 0.5 ns through MD (N,P,T). A similar procedure was followed for the MD of pure water at the different pressures. The analysis of the tetrahedrality of the H-bond network of water was based on the orientational order parameter,  $q$ , proposed by Chau and Hardwick,<sup>55</sup> although in the rescaled version introduced by Errington and Debenedetti.<sup>56</sup> This parameter is given by:

$$q = 1 - \frac{3}{8} \sum_{i=1}^3 \sum_{j=i+1}^4 \left( \cos \theta_{ij} + \frac{1}{3} \right)^2 \quad (1)$$

where  $\theta_{ij}$  is the angle formed by the lines joining the O atom of a given water molecule and those of its nearest neighbors,  $i$  and  $j$  ( $\leq 4$ ); the average value of  $q$  varies between 0 (ideal gas) and 1 (perfect tetrahedral H-bond network).<sup>56</sup> The parameter  $q$  decreases, therefore, for water molecules with a coordination number below four and for water molecules with distorted H-bonds, relative to a perfect tetrahedral network.

## III. RESULTS AND DISCUSSION

**Solvent Separated and Contact Ion Pairs.** The ion pair, radial distribution functions (RDFs) in solution at the different concentrations are depicted in Figure 1. As it may be seen, even at the highest concentrations, solvent separated ion pair configurations are dominant, and the coordination number is below 1, up to distances  $\sim 5.5$  Å. For the NaF and NaBr

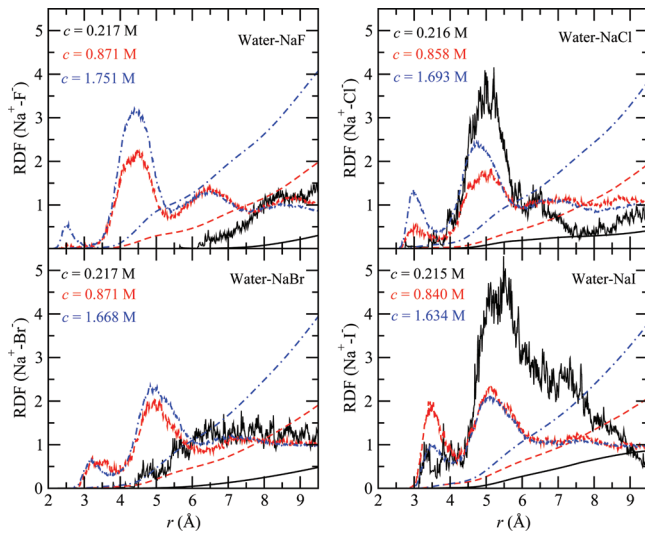


**Figure 1.** Sodium cation–halide anions RDF at the different concentrations studied and the respective coordination numbers (lines).

solutions at the lowest concentration, the cation and anion positions are not correlated, and for NaCl and NaI, although a prominent peak appears around 5.0 and 5.5 Å, respectively, the corresponding coordination number is much lower than 1. For the largest concentrations, a small peak appears at short distances for all of the salt solutions characteristic of contact ion pair configurations. The respective coordination number is however very low, and it should become significant only closer to saturation.

**Ionic Hydration and Structure.** Figure 2 (upper panel) shows the halide anions–oxygen RDFs. The loss of structure, reflected in the decrease of the height of the first and second peaks, in passing from the smallest to the largest anion is quite clear. The height of the first minimum of the RDFs also suggests significantly longer residence times of the water molecules near  $\text{F}^-$ , relative to the larger anions. The hydration of NaF leads to a significant volume contraction (see Table 1) associated to the strong electrostatic interactions between the  $\text{F}^-$  and the water molecules. The experimental apparent molar volume of aqueous NaF is negative contrary to the other sodium halides.<sup>57,58</sup> This volume contraction increased with concentration, and it emphasizes the importance of accounting for many body polarization effects in the description of  $\text{F}^-$ –water interactions. For  $\text{I}^-$ , the first minimum is only relatively well-defined at the lowest concentration, and it takes place at ~4.50 Å. For the larger concentrations, it shifts to ~4.65 and ~4.85 Å, respectively, although the minimum is not clear anymore, indicating a frequent passage of water molecules (O atoms) between the first two hydration shells. The larger value (4.85 Å) was used to define the outer limit of the first hydration shell for all concentrations, in the subsequent analysis of the water structure, because we are mostly interested in ionic long-range effects. Nonetheless, we verified that using the lower values does not change any of the results presented here.

The  $\text{Na}^+ - \text{O}$  RDFs for the different salt solutions at the highest concentration for each solution are plotted in Figure 2 (lower panel). The RDFs are rather similar, as expected, given the fact that contact ion pair configurations are not frequent and therefore the cation keeps its hydration shells nearly intact. Moreover, only for aqueous NaF and to a less extent for NaCl

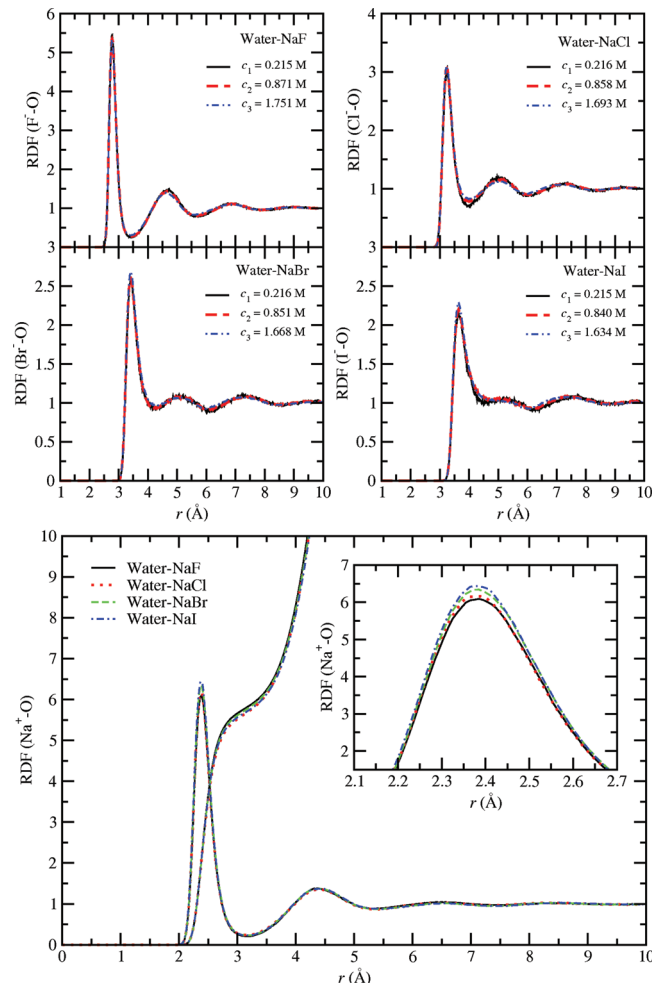


**Figure 2.** Upper panel: Halide anions–oxygen RDF at the different concentrations studied. Lower panel: Sodium cation–oxygen RDF for the different salts at the largest concentration for each salt.

is the cation first hydration shell expected to accommodate the counteranion, at larger concentrations, because the  $\text{Na}^+ - \text{X}^-$  first hydration shells fall at the outer edge of the  $\text{Na}^+ - \text{O}$  first hydration shell. On the other hand, a very low first minimum can be observed, which, like for  $\text{F}^-$ , suggests long residence times of water molecules in close interaction with  $\text{Na}^+$ . This observation is similar to that reported from neutron diffraction/EPRS experiments.<sup>16</sup> However, the  $\text{Na}^+$  hydration described by the AMOEBA potential depicts some differences from neutron diffraction/EPRS<sup>16</sup> results for NaCl solutions. The first peak maximum reported by Mancinelli et al.<sup>16</sup> is at 2.34 Å, and the coordination number of  $\text{Na}^+$  is 5.1 for a concentration (solute per water molecules) of 1:40, as compared to the value ~2.39 Å and a coordination number of 5.7 found here for the 1:32 NaCl aqueous solution. The position of the first minimum is, however, similar in both works, ~3.2 Å. For  $\text{Cl}^-$ , a first peak maximum located at 3.14 Å and a coordination number of 6.8 for the same concentration was reported from neutron diffraction/EPRS,<sup>16</sup> as opposed to the maximum at 3.23 Å and a coordination number of 8.2, found here. The position of the first minimum of the  $\text{Cl}^- - \text{O}$  RDF, ~4.1 Å, is also larger than the experimental value, 3.8 Å. The integration of the  $\text{Cl}^- - \text{O}$  RDF up to 3.8 Å gives in fact a coordination number very close, 6.9, to the experimental value. The position and minima of the peaks in the other halide anion–oxygen RDFs are also

larger than those reported from neutron diffraction/EPSR for potassium halide aqueous solutions at different concentrations.<sup>21</sup> Further, the coordination numbers (O atoms) obtained here increase in passing from the smallest to the largest anion,  $\text{F}^-$  (6.0),  $\text{Cl}^-$  (8.2),  $\text{Br}^-$  (9.6), and  $\text{I}^-$  (10.4), in contrast to those from neutron diffraction/EPSR<sup>21</sup> that are almost constant for the different anions, with values around 5.5–7.0 for the different halides and concentrations. The coordination numbers (H atoms) from the anion–hydrogen RDFs (not displayed here) at the largest concentrations are significantly lower,  $\text{F}^-$  (5.8),  $\text{Cl}^-$  (6.0),  $\text{Br}^-$  (5.8), and  $\text{I}^-$  (5.7); the respective first minima are  $\text{F}^-$  (2.6 Å),  $\text{Cl}^-$  (3.0 Å),  $\text{Br}^-$  (3.1 Å), and  $\text{I}^-$  (3.3 Å). These values are similar to the corresponding H coordination numbers found from neutron diffraction/EPSR,<sup>16,21</sup> ~5.5–6.0, and also almost constant. Thus, it is interesting to observe that despite the increase of the number of water molecules in the anionic first hydration shell, with the anionic size, each anion interacts directly with the same number of H atoms, ~6.

In Table 2, we summarize the values of the first, second, and third maxima and minima of the O–O RDF in pure water and

**Table 2. Position of the First, Second, and Third Maxima and Minima of the Ion–O Radial Distribution Functions at 298.15 K and 1 atm<sup>a</sup>**

| specie        | $R_{1\text{stmax}}$<br>(Å) | $R_{1\text{stmin}}^b$<br>(Å) <sup>b</sup> | $R_{2\text{ndmax}}$<br>(Å) | $R_{2\text{ndmin}}$<br>(Å) | $R_{3\text{rdmax}}$<br>(Å) | $R_{3\text{rdmin}}$<br>(Å) |
|---------------|----------------------------|---|----------------------------|----------------------------|----------------------------|----------------------------|
| O             | 2.81                       | 3.49                                      | 4.61                       | 5.67                       | 6.83                       | 7.97                       |
| $\text{Na}^+$ | 2.39                       | 3.18                                      | 4.40                       | 5.45                       | 6.55                       | 7.50                       |
| $\text{F}^-$  | 2.77                       | 3.42                                      | 4.63                       | 5.60                       | 6.85                       | 7.85                       |
| $\text{Cl}^-$ | 3.23                       | 4.05                                      | 5.08                       | 5.95                       | 7.15                       | 8.24                       |
| $\text{Br}^-$ | 3.42                       | 4.30                                      | 5.15                       | 6.00                       | 7.22                       | 8.40                       |
| $\text{I}^-$  | 3.64                       | 4.50 <sup>c</sup>                         | 5.20                       | 6.10                       | 7.39                       | 8.69                       |

<sup>a</sup>The respective values for the O–O pair correlation function in neat water are also reported. <sup>b</sup>The coordination numbers (O atoms) in water and in the salt solutions at the respective highest concentration, except for  $\text{I}^-$ , corresponding to the RDFs first minimum, are: O (5.3),  $\text{Na}^+$  (5.7–5.8),  $\text{F}^-$  (6.0),  $\text{Cl}^-$  (8.2),  $\text{Br}^-$  (9.6), and  $\text{I}^-$  (10.4). The coordination numbers do not change significantly for the concentrations studied, except for  $\text{I}^-$ . <sup>c</sup>The first peak minimum at 4.5 Å for  $\text{I}^-$  corresponds to the lowest concentration where the first minimum is better defined. This minimum shifts to larger distances with concentration, and at the largest concentration,  $c_3$ , the minimum takes place at ~4.85 Å with a coordination number ~13.6.

of the ion–oxygen RDFs. The coordination numbers (O atoms) for pure water and for the sodium cation and the halide anions are also reported.

**Tetrahedral Orientational Order of Water.** The coordination number (O atoms) of water found in this work was 5.3 (Table 2), while the coordination number obtained from the O–H RDF (not displayed here) was 3.9 with the O–H RDF first minimum at ~2.44 Å. The water molecules in direct interaction with the ions in solution have a smaller number of water molecules in their first hydration shell than those not in direct interaction with the ions, and water molecules in pure water. The water number density around these molecules is therefore lower, and if the water partial RDFs in the salt solutions are not corrected for inhomogeneity, the height of the peaks decreases, relative to neat water. On the other hand, the water molecules in direct interaction with the ions have a lower value of  $q$ . Hence, to probe water structure perturbations in the ionic solutions, relative to neat water, we

must discard the water molecules in close interaction with the ions. Here, we excluded the water molecules in the first ionic hydration shell. Notice however that for the largest anions, the water molecules at the outer edge of the first ionic hydration shell are not in direct interaction with the anions and can form four water–water H-bonds. We consider first the individual effect of the halide anions and  $\text{Na}^+$  in the tetrahedrality of the H-bond network of liquid water.

**Second Ionic Hydration Shell.** Figure 3 (upper panel) shows the distribution of the parameter  $q$  and the respective

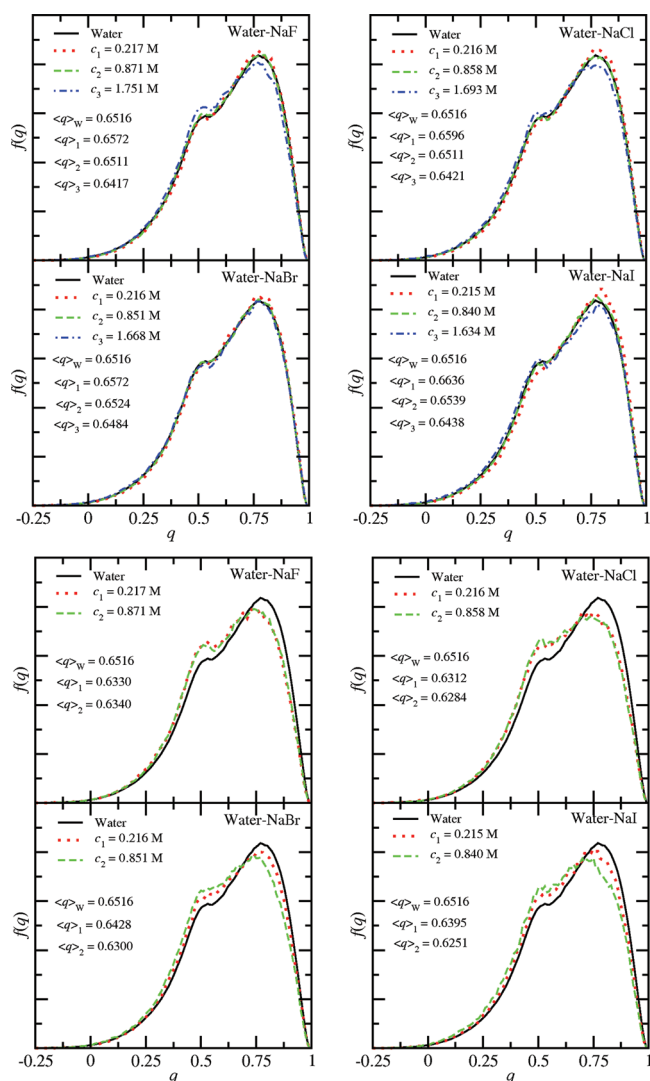


**Figure 3.** Distribution of the parameter  $q$  in pure water and for the different salt solutions. Upper panel: Water molecules in the second hydration shell of the halide anions. Lower Panel: Water molecules in the second hydration shell of the sodium cation. The respective average values of  $q$  are given.

average values, for pure water and for the water molecules in the second anionic hydration shell, for the different solutions. The tetrahedrality parameter was calculated only for those water molecules in the second anionic hydration shell, and, concomitantly, not at a distance smaller than the third hydration shell minimum of  $\text{Na}^+$  (Table 2). The water molecules excluded in each configuration are still “seen” by the other water molecules, only not just considered as origins to compute  $q$ . For the concentrations corresponding to more than

a single ionic pair,  $q$  was averaged over the water molecules in the second hydration shell of each anion. Thus, for instance, for the NaF aqueous solution at the highest concentration (1.751 M), all of the water molecules in the region defined by  $3.415 \text{ \AA} < r_{\text{F}^- \text{O}} < 5.600 \text{ \AA}$  and  $r_{\text{Na}^+ \text{O}} > 7.500 \text{ \AA}$ , for each of the eight  $\text{F}^-$  anions, were considered. This way we eliminate as much as possible the hypothetical long-range influence of the cation in the distribution of  $q$  that characterizes a specific anionic effect. The distribution of  $q$  for pure water is bimodal as expected,<sup>56</sup> depicting a maximum at  $q = 0.77$  and a shoulder with a maximum at a lower value of  $q = 0.53$ , reflecting the existence of water molecules more structured (near tetrahedral) and water molecules with broken and/or distorted H-bonds. For the water molecules in the second hydration shell of the different anions, it can be seen that the anions enhance the tetrahedrality of water at the lowest concentration, and (apparently) reduce the average value of  $q$  at the largest concentration studied. However, and contrary to its position in the Hofmeister series,  $\text{I}^-$  induces the largest increase in  $q$ , slightly shifting the maximum of the distribution to a larger value,  $q = 0.80$ , as well as increasing its height, and shifting downward the shoulder around  $q = 0.5$ , relative to neat water. A similar effect, although more pronounced, was recently reported regarding the hydrophobic hydration of benzene in water.<sup>59</sup> The size and the low charge density of  $\text{I}^-$  leads to a significantly less rigid first ionic hydration shell, which appears to further promote this tetrahedrality enhancement of the water molecules, relative to the other halide anions. On the other hand,  $\text{F}^-$ , which is at the opposite end of the Hofmeister series, and classified as a strong structure maker or kosmotrope, induces a smaller increase of  $q$ . Here, the effect of a rather rigid first hydration shell, associated to a volume contraction of the system, appears to debilitate its structure-making ability in the second shell. We note that the  $\text{F}^-$  reputation as a strong structure maker is commonly based on its first hydration shell structure and solvation enthalpy.<sup>5</sup> For higher concentrations, the tetrahedrality decreases, and at the largest concentration studied for each salt, the average value of  $q$  is already lower than that found for neat water. This suggests that at large concentrations, the H-bond network is already significantly perturbed by the cations and anions in such a way that the overall effect is a decrease of the tetrahedrality of water, which extends inside the anions' second hydration shell. This effect is further discussed when we consider the water structure in the third hydration shell. Figure 3 (lower panel) depicts analogous curves for the water molecules in the second hydration shell of  $\text{Na}^+$ . The results for the largest concentrations are omitted because the number of water molecules is already too low, especially for the NaI solution. Notice that in this case the third anionic hydration shell minima (Table 2) are used to further sample the water molecules included in the calculation of  $q$ . The effect here is opposite to that observed for the anions. Thus,  $\text{Na}^+$  acts as a strong chaotrope, in terms of the measured orientational order. Again, this is contrary to the cation position in the cationic Hofmeister series. A neutron diffraction/EPSR study by Mancinelli et al.<sup>16</sup> on solutions of NaCl and KCl at different concentrations showed that water molecules in the  $\text{Na}^+$  hydration shell were tightly coordinated to the cation, and  $\text{Na}^+$  was a stronger structure breaker than  $\text{K}^+$ , relative to the water structure. The distribution of  $q$  for the different salt solutions clearly supports this conclusion for water molecules in the  $\text{Na}^+$  second hydration shell.

These results suggest therefore that if the parameter  $q$  is taken as a measure of the water structure, then the classification of anions and cations in kosmotropes/chaotropes does not follow their position in the Hofmeister series. Moreover, the overall structure-making effect of the anions upon the second anionic hydration water molecules is relatively small, while  $\text{Na}^+$  disrupts significantly the tetrahedrality of water in the second hydration shell.

**Third Ionic Hydration Shell.** We now discuss the effect of the anions and cations beyond the second hydration shell. Figure 4 depicts the distribution of  $q$  for the second and third anionic hydrations shells of the halide anions, for the distinct concentrations. A similar procedure was used to sample the third anionic hydration shells; that is, the water molecules sampled are in the third anionic hydration shell and not at a distance smaller than the third hydration shell minimum of the  $\text{Na}^+$  cation. The results show that the tetrahedrality of the water molecules decreases in passing from the second to the third hydration shell. For the lowest concentrations, this means that water in the third anionic hydration shell resembles more pure water than the water molecules in the second hydration shell. This result is expected, and we can conclude that the effect of the anions is limited to the second hydration shell. However, for the largest concentrations, the decrease of tetrahedrality in passing from the second to the third hydration shell maintains, even though water in the second hydration shell is already less tetrahedral than pure water. Further insight on this result can be gained by analyzing the tetrahedrality of water in the cation's third hydration shell. The results for the lower concentrations for the different salts are depicted in Figure 5. For  $\text{Na}^+$ , an opposite behavior is observed, and the tetrahedrality of water molecules increases with the distance to the cation, as expected. For the lowest concentration, the effect of  $\text{Na}^+$  on the water tetrahedrality is also mostly constrained to the second hydration shell. However, at the intermediate concentration, it can be seen that  $q$  is lower than for pure water and in fact very similar to the values found for the third hydration shell of the anions, at the same concentration. This suggests that at these larger concentrations, water can no longer recover its normal tetrahedral orientational order. Because the cation and the anions' specific effects on the water molecules, in the respective second hydration shells, are opposite, it appears that the overall disruption of tetrahedrality, which extends to the anionic second hydration shells, results from the stronger structure breaker effect observed for  $\text{Na}^+$ . Thus, despite that water molecules up to the third hydration shell of  $\text{Na}^+$  are excluded in the calculation of  $q$  for water molecules in the anionic hydration shells, at large salt concentrations, when hydration shells overlap more frequently, the  $\text{Na}^+$  hydration atmosphere significantly influences the structure of water in the anionic hydration layers.

We should note that if the notion of kosmotrope/chaotrope is applied to the first ionic hydration shell, then  $\text{Na}^+$  and the halide anions follow their normal classification, because both  $\text{Na}^+$  and  $\text{F}^-$  are tightly bound to water molecules in the first hydration shell, while  $\text{I}^-$  exhibits a significantly less structured hydration shell (Figure 2). However, our results show that this local structuring cannot be extrapolated to the perturbations on the water H-bond network tetrahedrality in salt solutions, as this classification implies.

**Salt and Pressure Effects.** Here, we focus on both the pressure and the overall effect of sodium halides in the water structure. At room temperature and high pressures, the

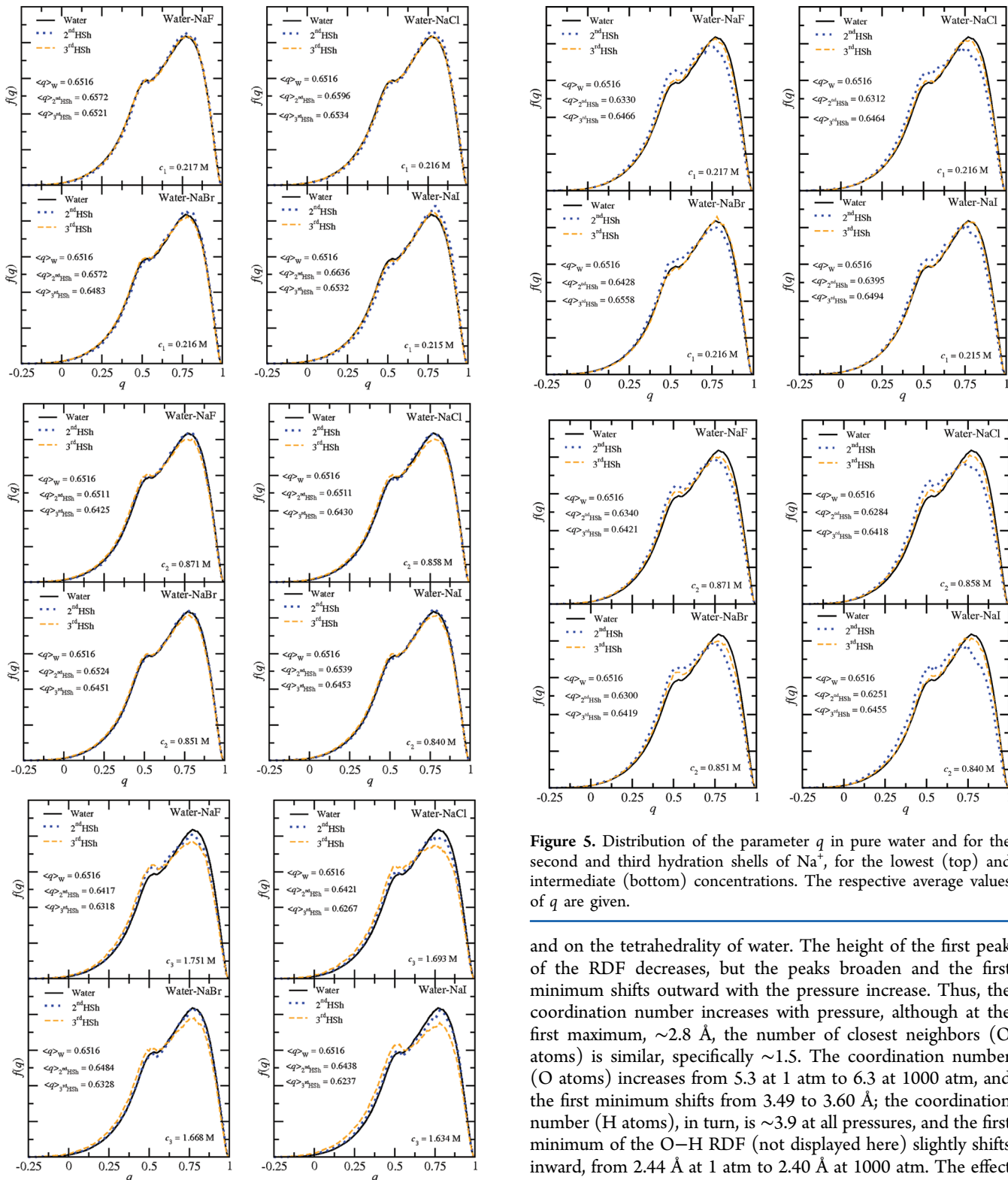


**Figure 4.** Distribution of the parameter  $q$  in pure water and for the second and third hydration shells of the halide anions, from the lowest to the highest concentration, from top to bottom, respectively. The respective average values of  $q$  are given.

coordination number of water increases and water is less structured. Thus, the water H-bonds either break or bend, or both, diminishing the overall tetrahedrality of the network. Figure 6 displays the effect of the pressure on the O–O RDF

**Figure 5.** Distribution of the parameter  $q$  in pure water and for the second and third hydration shells of  $\text{Na}^+$ , for the lowest (top) and intermediate (bottom) concentrations. The respective average values of  $q$  are given.

and on the tetrahedrality of water. The height of the first peak of the RDF decreases, but the peaks broaden and the first minimum shifts outward with the pressure increase. Thus, the coordination number increases with pressure, although at the first maximum,  $\sim 2.8$  Å, the number of closest neighbors (O atoms) is similar, specifically  $\sim 1.5$ . The coordination number (O atoms) increases from 5.3 at 1 atm to 6.3 at 1000 atm, and the first minimum shifts from 3.49 to 3.60 Å; the coordination number (H atoms), in turn, is  $\sim 3.9$  at all pressures, and the first minimum of the O–H RDF (not displayed here) slightly shifts inward, from 2.44 Å at 1 atm to 2.40 Å at 1000 atm. The effect of pressure on the orientational order of water, on the other hand, is a clear disruption of the tetrahedrality of the H-bonds.

Figure 7 depicts the O–O RDFs for the salt solutions at the distinct concentrations, calculated for all of the water molecules (upper panel), and excluding the molecules in the first (middle panel) and in the first and second (lower panel) hydration shells of the anions and  $\text{Na}^+$ . Note that like for the calculation of  $q$ , the water molecules excluded as origins are still “seen” by the other molecules in the system. The effect of not excluding the water molecules in the first ionic hydration shells is the

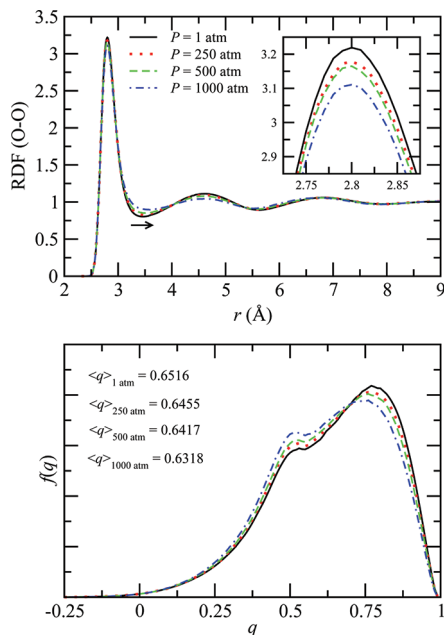


**Figure 6.** Water oxygen–oxygen RDF for pure water at different pressures (top) and the respective tetrahedrality parameter distributions and average values (bottom).

decrease of the height of the peaks, previously discussed, as well as a shift of the first minimum to larger distances, similar to that observed in water at high pressures. Thus, the average number of water molecules at the first peak maximum decreases with the concentration increase, but the coordination number actually increases, because of the shift of the first minimum to larger distances. The exclusion of the water molecules in the first ionic hydration shells leads to the inversion of the height of the first peak with concentration, while it still shifts slightly to larger distances. Here, the ions still influence the height of the peaks, although only at distances larger than the lowest ion–oxygen first minimum ( $3.18 \text{ \AA}$  for  $\text{Na}^+$ , Table 2). Note that these RDFs are not for the water molecules in the second hydration shell of the cations and anions, but for all of the water molecules beyond the first ionic hydration shells.

The height of the peaks decreases and the RDFs are closer to that of pure water, as expected, when the water molecules of both the first and the second hydration layers are excluded (Figure 7, lower panel). For the  $\text{NaF}$  solution, a new inversion of the height of the first peak takes place, relative to pure water, which results, in part, from the larger number density of water in the  $\text{NaF}$  solution. For the other salts, the number density decreases relative to neat water, and therefore we expect higher peaks relative to pure water. The difference between the O–O RDFs plotted in the middle and lower panels of Figure 7 reflects the salt effects on the average structure of water molecules in the second ionic hydration shells. The only significant difference, relative to pure water, is a small increase of the height of the first peak and a slight shift outward of the first peak. This observation could perhaps be interpreted as an enhancement of the water structure, contrary to the effect of pressure. However, even though water is apparently more structured in the salt solutions, the O–O RDFs do not provide insight on the tetrahedrality of the H-bond network of water. Hence, we now discuss the distribution of  $q$  obtained by excluding the water molecules in the first hydration shell of the cations and anions in solution. The average effect of the distinct

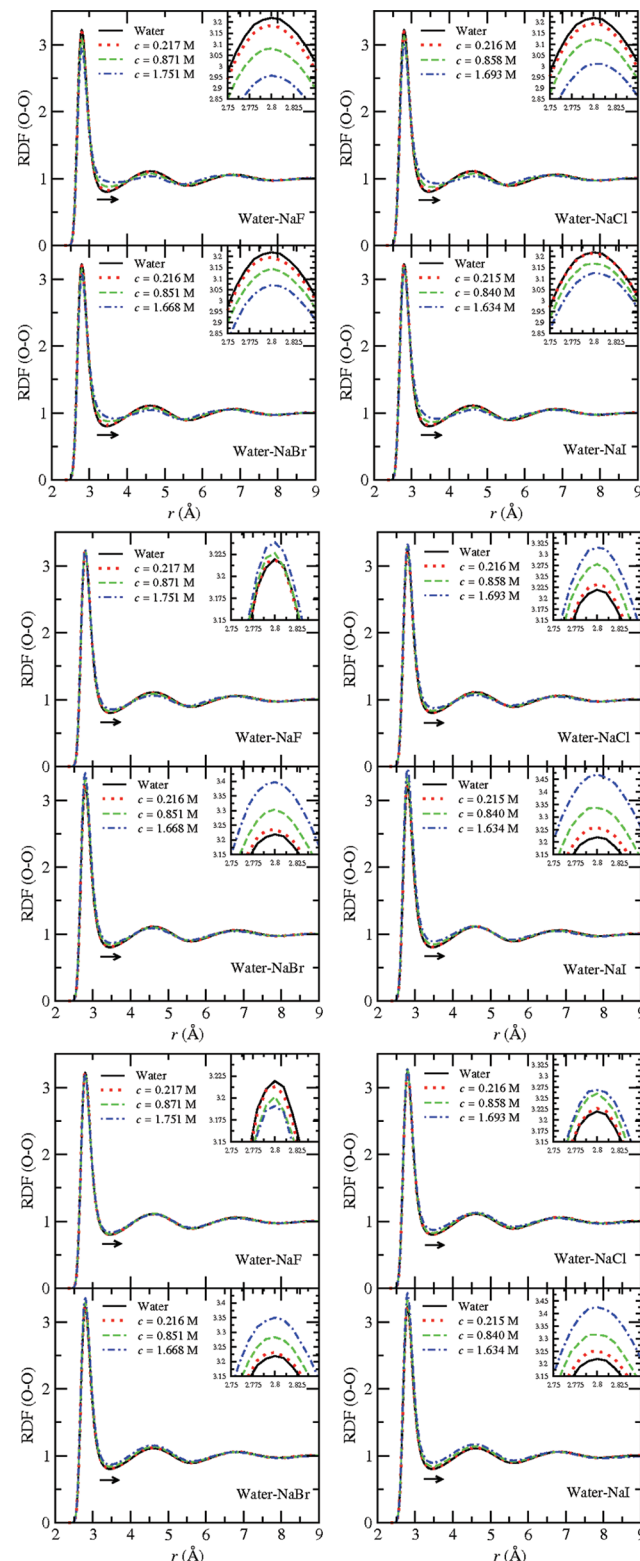


**Figure 7.** Water oxygen–oxygen RDF in pure water and in the salt solutions. From top to bottom, respectively, no water molecules excluded, exclusion of the water molecules in the first ionic (anions and cations) hydration shells and exclusion of the water molecules in the first and second ionic (anions and cations) hydration shells.

salt at the lowest concentration is almost nonexistent (Figure 8). This means the cation and anion individual effects cancel out to a large extent. At larger concentrations, the salts could be

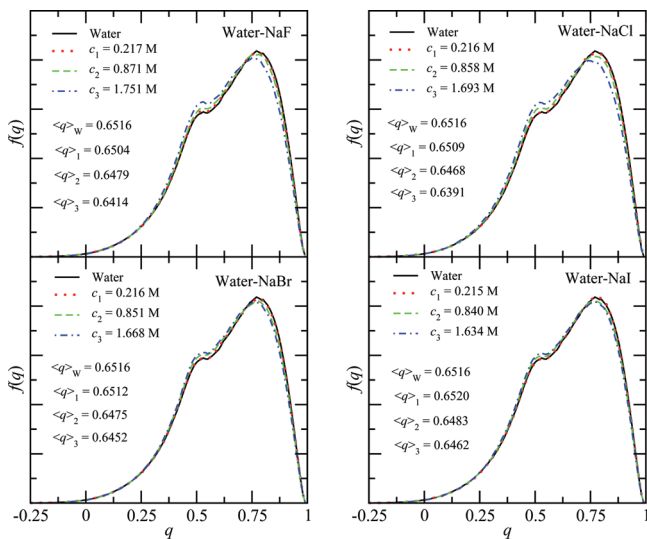


**Figure 8.** Distribution of the parameter  $q$  in pure water and for the salt solutions excluding the water molecules in the first ionic (anions and cations) hydration shells.

classified as chaotropes, in agreement with the previous discussion on the dominant role of  $\text{Na}^+$ , but in disagreement with the common differentiation of these salts in kosmotropes and chaotropes. On the other hand, the effect observed with increasing concentration is very similar to that for water at high pressures. For the concentrations studied here, we can see that the equivalent pressure is below 1000 atm for all of the salts. Thus, despite the differences between the O–O RDFs for pure water at high pressures and water in salt solutions, the average tetrahedrality of the H-bond network appears to be changed in a very similar way. This is in keeping with the conclusions of Mancinelli et al.,<sup>15</sup> although not based on the same observations. Thus, we do not observe an inner shift of the second O–O peak neither for water at high pressures nor for the salt solutions, which supported the authors' conclusions. Nonetheless, we should emphasize that only the average tetrahedrality is similar, because the anions and cations exert different perturbations on the water H-bond network.

#### IV. CONCLUDING REMARKS

The tetrahedrality of the H-bond network of water in sodium halide aqueous solutions at different concentrations, and room temperature and pressure, was studied through molecular dynamics. The present results suggest that the kosmotropes/chaotropes classification of ions, often also associated to the dynamics of water in the first ionic hydration shell, does not explain the ionic effects on the H-bond network of water, outside the first coordination sphere. In this sense, the structure of the water H-bond network in salt solutions is not correlated with the position of the ions in the respective Hofmeister series. Even though in this work the dynamics of water has not been addressed, it is likely, at least at high concentrations, that the disruption of the tetrahedrality of the H-bond network of water has some impact on the dynamic properties of salt solutions. However, in the light of the results reported here, the decrease of the self-diffusion of water and the increase of the viscosity of sodium halide solutions with concentration, at room temperature, should be primarily related to the ion–water interactions and the dynamics of water, in the first hydration shell, as expected, because the average perturbation, induced by the

cation and the anions, in the water structure is relatively small. Finally, regarding the effect of long-range ionic-induced water structure perturbations on the solubility of proteins, our results also indicate that these should not be significant, and should be overcome by water local interactions with hydrophilic and hydrophobic amino acid groups. Thus, ion–protein interactions are likely to be much more significant than ion-induced long-range water structure perturbations, in agreement with the current view about Hofmeister ion effects on protein stability.

#### ■ AUTHOR INFORMATION

##### Corresponding Author

\*E-mail: ngalamba@ciif.fc.ul.pt.

##### Notes

The authors declare no competing financial interest.

#### ■ ACKNOWLEDGMENTS

N.G. gratefully acknowledges financial support from Fundação para a Ciência e a Tecnologia from Portugal through the project PTDC/QUI-QUI/113376/2009.

#### ■ REFERENCES

- Zhang, Y.; Cremer, P. S. *Curr. Opin. Chem. Biol.* **2006**, *10*, 658.
- Marcus, Y. *Chem. Rev.* **2009**, *109*, 1346.
- Kunz, W.; Lo Nostro, P.; Ninham, B. W. *Curr. Opin. Colloid Interface Sci.* **2004**, *9*, 1.
- Bakker, H. J. *Chem. Rev.* **2008**, *108*, 1456.
- Ohtaki, H.; Radnai, T. *Chem. Rev.* **1993**, *93*, 1157.
- Collins, K. D.; Neilson, G. W.; Enderby, J. E. *Biophys. Chem.* **2007**, *128*, 95.
- Bakker, H. J.; Kropman, M. F.; Omata, A. W. *J. Phys.: Condens. Matter* **2005**, *17*, S3215.
- Batchelor, J. D.; Olteanu, A.; Tripathy, A.; Pielak, G. J. *J. Am. Chem. Soc.* **2004**, *126*, 1958.
- Kanno, H.; Yonehama, K.; Somraj, A.; Yoshimura, Y. *Chem. Phys. Lett.* **2006**, *427*, 82.
- Kropman, M. F.; Bakker, H. J. *Science* **2001**, *291*, 2118.
- Kropman, M. F.; Bakker, H. J. *J. Chem. Phys.* **2001**, *115*, 8942.
- Kropman, M. F.; Bakker, H. J. *J. Am. Chem. Soc.* **2004**, *126*, 9135.
- Kropman, M. F.; Nienhuys, H.-K.; Bakker, H. J. *Phys. Rev. Lett.* **2002**, *88*, 077601.
- Leberman, R.; Soper, A. K. *Nature* **1995**, *378*, 364.
- Mancinelli, R.; Botti, A.; Bruni, F.; Ricci, M. A.; Soper, A. K. *Phys. Chem. Chem. Phys.* **2007**, *9*, 2959.
- Mancinelli, R.; Botti, A.; Bruni, F.; Ricci, M. A.; Sopper, A. K. *J. Phys. Chem. B* **2007**, *111*, 13570.
- Omata, A. W.; Kropman, M. F.; Woutersen, S.; Bakker, H. J. *Science* **2003**, *301*, 347.
- Omata, A. W.; Kropman, M. F.; Woutersen, S.; Bakker, H. J. *J. Chem. Phys.* **2003**, *119*, 12457.
- Perera, P. N.; Browder, B.; Ben-Amotz, D. *J. Phys. Chem. B* **2009**, *113*, 1805.
- Smith, J. D.; Saykally, R. J.; Geissler, P. L. *J. Am. Chem. Soc.* **2007**, *129*, 13847.
- Soper, A. K.; Weckstrom, K. *Biophys. Chem.* **2006**, *124*, 180.
- Westh, P.; Kato, H.; Nishikawa, K.; Koga, Y. *J. Phys. Chem. A* **2006**, *110*, 2072.
- Imberti, S.; Botti, A.; Bruni, F.; Cappa, G.; Ricci, M. A.; Soper, A. K. *J. Chem. Phys.* **2005**, *122*.
- Bouazizi, S.; Nasr, S. *J. Mol. Liq.* **2011**, *162*, 78.
- Fayer, M. D.; Moilanen, D. E.; Wong, D.; Rosenfeld, D. E.; Fenn, E. E.; Park, S. *Acc. Chem. Res.* **2009**, *42*, 1210.
- Carrillo-Tripp, M.; Saint-Martin, H.; Ortega-Blake, I. *J. Chem. Phys.* **2003**, *118*, 7062.

- (27) Hribar, B.; Southall, N. T.; Vlachy, V.; Dill, K. A. *J. Am. Chem. Soc.* **2002**, *124*, 12302.
- (28) Ikeda, T.; Boero, M.; Terakura, K. *J. Chem. Phys.* **2007**, *126*, 034501.
- (29) Kim, J. S.; Yethiraj, A. *J. Phys. Chem. B* **2008**, *112*, 1729.
- (30) Lyubartsev, A. P.; Laasonen, K.; Laaksonen, A. *J. Chem. Phys.* **2001**, *114*, 3120.
- (31) Tongraar, A.; Liedl, K. R.; Rode, B. M. *J. Phys. Chem. A* **1998**, *102*, 10340.
- (32) Galamba, N.; Cabral, B. J. C. *J. Phys. Chem. B* **2009**, *113*, 16151.
- (33) Chandrasekhar, J.; Jorgensen, W. L. *J. Chem. Phys.* **1982**, *77*, 5080.
- (34) Chandrasekhar, J.; Spellmeyer, D. C.; Jorgensen, W. L. *J. Am. Chem. Soc.* **1984**, *106*, 903.
- (35) Zhu, S. B.; Robinson, G. W. *J. Chem. Phys.* **1992**, *97*, 4336.
- (36) Chandra, A. *Phys. Rev. Lett.* **2000**, *85*, 768.
- (37) Lightstone, F. C.; Schwegler, E.; Hood, R. Q.; Gygi, F.; Galli, G. *Chem. Phys. Lett.* **2001**, *343*, 549.
- (38) Holzmann, J.; Ludwig, R.; Geiger, A.; Paschek, D. *Angew. Chem., Int. Ed.* **2007**, *46*, 8907.
- (39) Koneshan, S.; Rasaiah, J. C.; Lynden-Bell, R. M.; Lee, S. H. *J. Phys. Chem. B* **1998**, *102*, 4193.
- (40) Chialvo, A. A.; Simonson, J. M. *J. Mol. Liq.* **2004**, *112*, 99.
- (41) Impey, R. W.; Madden, P. A.; McDonald, I. R. *J. Phys. Chem.* **1983**, *87*, 5071.
- (42) Gallo, P.; Corradini, D.; Rovere, M. *Phys. Chem. Chem. Phys.* **2011**, *13*, 19814.
- (43) Laage, D.; Hynes, J. T. *Proc. Natl. Acad. Sci. U.S.A.* **2007**, *104*, 11167.
- (44) Corradini, D.; Rovere, M.; Gallo, P. *J. Phys. Chem. B* **2011**, *115*, 1461.
- (45) Grossfield, A.; Ren, P. Y.; Ponder, J. W. *J. Am. Chem. Soc.* **2003**, *125*, 15671.
- (46) Tobias, D. J.; Hemminger, J. C. *Science* **2008**, *319*, 1197.
- (47) Hofmeister, F. *Arch. Exp. Pathol. Pharmakol.* **1888**, *24*, 247.
- (48) Omta, A. W.; Kropman, M. F.; Woutersen, S.; Bakker, H. J. *Science* **2003**, *301*, 347.
- (49) Zangi, R. *J. Phys. Chem. B* **2010**, *114*, 643.
- (50) Ren, P. Y.; Ponder, J. W. *J. Comput. Chem.* **2002**, *23*, 1497.
- (51) Ren, P. Y.; Ponder, J. W. *J. Phys. Chem. B* **2003**, *107*, 5933.
- (52) Ponder, J. W. *TINKER: Software Tools for Molecular Design*, S.1; Washington University School of Medicine: Saint Louis, MO, 2010.
- (53) Beeman, D. *J. Comput. Phys.* **1976**, *20*, 130.
- (54) Berendsen, H. J. C.; Postma, J. P. M.; Vangunsteren, W. F.; Dinola, A.; Haak, J. R. *J. Chem. Phys.* **1984**, *81*, 3684.
- (55) Chau, P. L.; Hardwick, A. J. *Mol. Phys.* **1998**, *93*, 511.
- (56) Errington, J. R.; Debenedetti, P. G. *Nature* **2001**, *409*, 318.
- (57) Millero, F. J. *J. Phys. Chem.* **1967**, *71*, 4567.
- (58) Millero, F. J. *J. Phys. Chem.* **1969**, *73*, 2417.
- (59) Mateus, M. P. S.; Galamba, N.; Costa Cabral, B. J. *J. Chem. Phys.* **2012**, *136*, 014507.